Electronic Supplementary Information

Engineering semiconductor quantum dots for co-upcycling of CO_2 and biomass-derived alcohol

Lin-Xing Zhang[a], Zi-Rong Tang[a], Ming-Yu Qi*[ab] and Yi-Jun Xu*[a]

[a]*College of Chemistry, State Key Laboratory of Photocatalysis on Energy and Environment, Fuzhou University, Fuzhou, 350116, P.R. China*

[b]*Institute of Fundamental and Frontier Sciences, University of Electronic Science and Technology of China, Chengdu, 611731, P.R. China*

**To whom correspondence should be addressed. Tel. /Fax: +86 591 22865836;*

E-mail: myqi@uestc.edu.cn; yjxu@fzu.edu.cn

Content list

Experimental procedures

Characterization

The morphology and element distribution of samples were analyzed by transmission electron microscopy (TEM), high-resolution TEM (HRTEM) and elemental mapping analysis using a JEOL model JEM-2100F instrument supported by Shiyanjia Lab "www.shiyanjia.com". The morphology of the samples was analyzed by scanning electron microscopy (SEM) on a FEI Nova NANO-SEM 230 spectrophotometer. The crystal structure of the sample was measured by X-ray diffraction (XRD) on a Rigaku Miniflex diffractometer with Cu Kα radiation in the 2θ range from 10 to 80 °. X-ray photoelectron spectroscopy (XPS) was employed to analyze the surface chemical state and composition of the sample (Thermo Scientific K-Alpha). All binding energies were calibrated by the C 1s peak at 284.60 eV. The light absorption properties of the samples were assessed by ultraviolet-visible diffuse reflectance spectroscopy (DRS) on an UV-vis spectrophotometers (Thermo Scientific Evolution 200 Series), with $BaSO_4$ as a reflectance standard. Fourier transform infrared (FTIR) spectroscopy was performed on a Nicolet iS50 FT-IR spectrophotometer with a resolution of 4 cm^{-1}. For in-situ FT-IR measurement, 20 mg of sample powders were placed onto KBr and 200 μL CH_3CN containing 0.1 mmol of furfuryl alcohol was added. The reaction system was purged with CO_2 for 20 min and irradiated with a 300 W Xe lamp. Dynamic light scattering (DLS) was utilized to assess the particle size of quantum dots (QDs) using the Zetasizer Nano-ZS90 instrument. The photoluminescence (PL) spectra and time-resolved PL (TRPL) decay plots of the samples were analyzed using the Edinburgh Analytical Instrument FLS980 series fluorescence spectrophotometer. Electron paramagnetic resonance (EPR) spectroscopy measurements were performed using a Bruker A300 EPR spectrometer. For typical EPR measurements, sample (20 mg) was dispersed in a 10 mL of CH_3CN mixed solution containing furfuryl alcohol (0.1 mmol) and 5, 5-dimethyl-1-pyrroline N-oxide (DMPO, 0.1 mmol). Then, the suspension was injected into a glass capillary tube, and placed in a sealed glass tube under an Ar atmosphere, and irradiated with 300 W Xe arc lamp at room temperature. The thermogravimetric (TG) analysis was performed using a TGA/DSC apparatus (METTLER TGA/DSC 3+) in an N_2 atmosphere. A chemisorption analyzer (Micromeritics Autochem 2920) was used to conduct CO_2 temperature-programmed-desorption (TPD) measurements. The isotope tracing experiment was examined on the Shimadzu QP-2020 gas chromatograph-mass spectrometry (GC-MS)

using an SH-Molecular Sieve 5A PLOT column.

Photoelectrochemical measurements

The photoelectrochemical and electrochemical measurements were performed using the electrochemical work station (MUTI AUTOLAB M204) in a three-electrode configuration. The Pt sheet served as the counter electrode, a saturated Ag/AgCl electrode as the reference electrode, and the working electrode was fluorine doped tin oxide (FTO) glass. Initially, transparent tape was applied to safeguard the FTO glass boundary, limiting the exposed area of the working electrode to 0.25 cm^2. Subsequently, 20 mg of the sample was thoroughly dispersed in a mixture of 500 μL of N, N-dimethylformamide (DMF) and 50 μL of Nafion membrane solution by ultrasonic treatment, resulting in a slurry. The slurry (20 μL) was coated on the pre-treated FTO glass and dried at 60 ℃ for 1 h to enhance adhesion. The transient photocurrent measurement was conducted in a 0.2 M Na_2SO_4 aqueous solution without an applied voltage bias under the UV-vis light irradiation. Additionally, the cyclic voltammetry (CV) curves were measured in a 0.2 M Na_2SO_4 aqueous solution. Cathodic linear sweep voltammetry (LSV) tests were performed in either Ar-saturated or CO_2-saturated Na_2SO_4 solution without light. The electrochemical impedance spectroscopy (EIS) measurement was carried out in a 0.5 M KCl solution including 0.01 M $K_3[Fe(CN)_6]/K_4[Fe(CN)_6]$. Mott-Schottky plots were obtained at frequencies of 500 and 1000 Hz with a bias potential ranging from −1 to 2 V *vs.* Ag/AgCl.

Photocatalytic recycling tests

To evaluate the photocatalytic stability and recyclability of the catalyst, recycling tests were carried out. The specific experimental steps were as follows. At the end of the first photocatalytic reaction, the catalyst was washed three times with CH_3CN and dried overnight at 60 ℃. Then, 10 mL of CH_3CN containing 0.1 mmol of furfuryl alcohol was added to the used catalyst for the second cycle test. Subsequent recycle tests were performed in a similar manner.

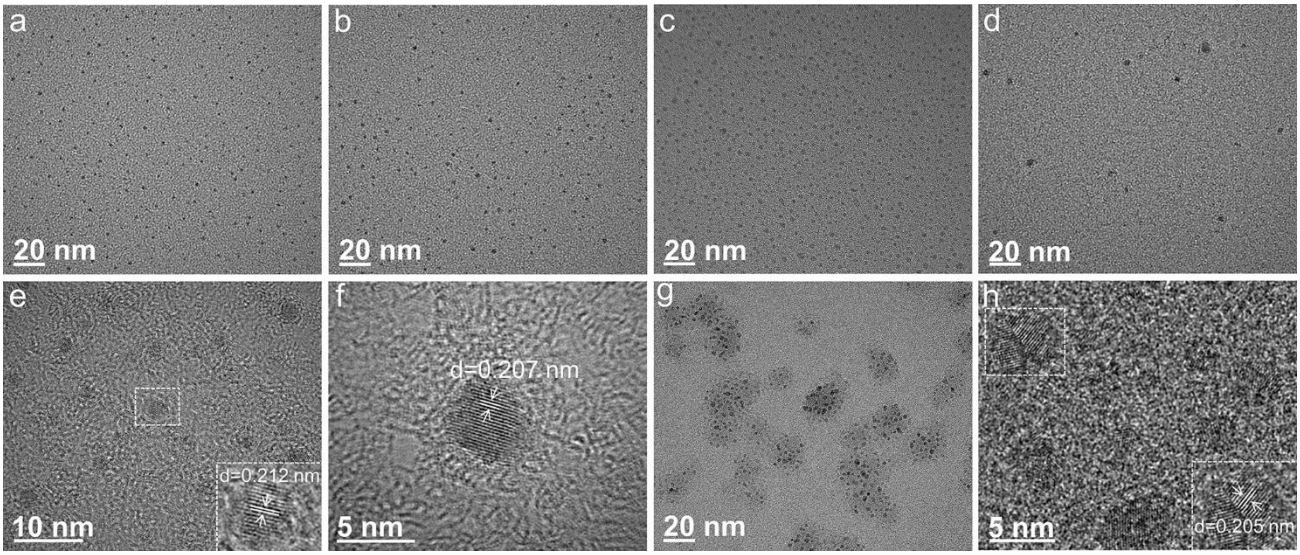

Fig. S1. TEM images of (a) CdSe QDs, (b) CdSe/1CdS QDs, (c) CdSe/3CdS QDs and (d) CdSe/7CdS QDs. HRTEM images of (e) CdSe/1CdS QDs and (f) CdSe/7CdS QDs. (g) TEM and (h) HRTEM images of CdS QDs.

Note: As depicted in **Fig. S1a-d**, the size of the CdSe/xCdS QDs (x = 1, 3 and 7) increases with the thickness of the CdS shell, where x represents approximately x atomic layers of CdS shell. The lattice fringes of CdSe/1CdS QDs (0.212 nm), CdSe/3CdS QDs (0.210 nm), and CdSe/7CdS QDs (0.207 nm) gradually converge towards those of CdS QDs (0.205 nm). Furthermore, the QDs sizes measured by DLS (**Fig. S2**) are consistent with TEM results, confirming the successful synthesis of core/shell structure QDs.[1]

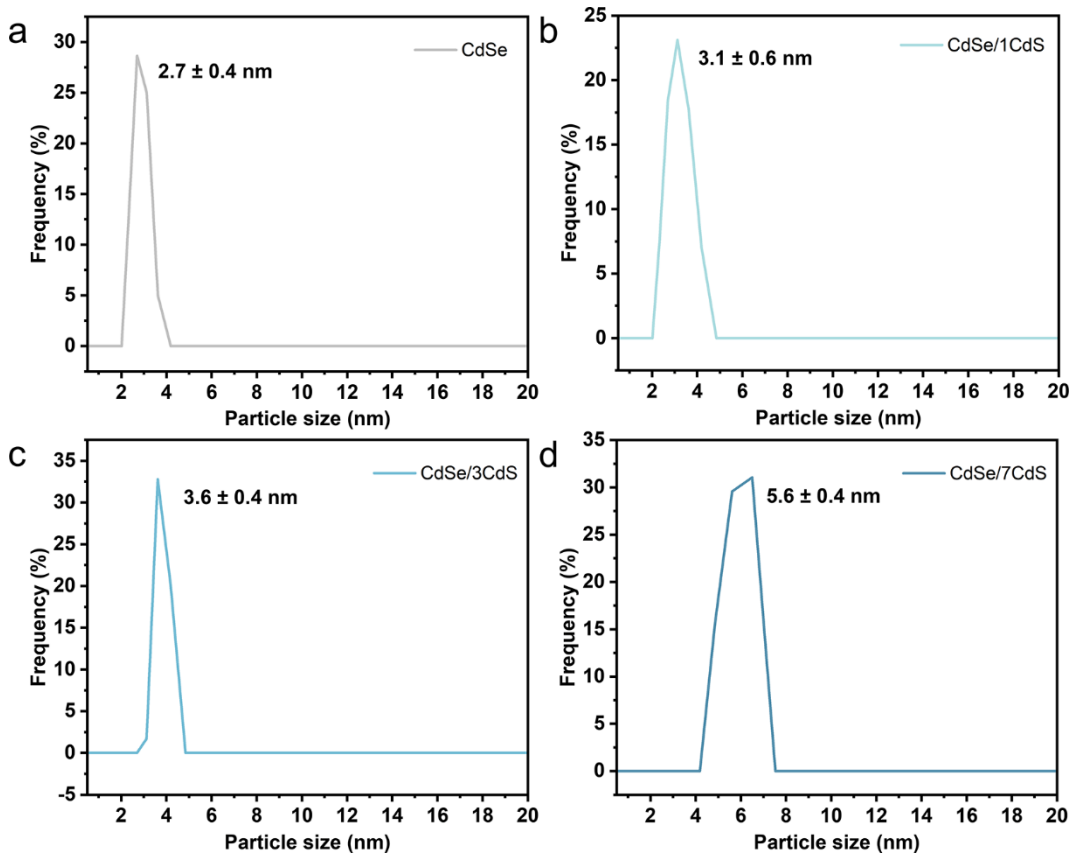

Fig. S2. Size distribution of (a) CdSe QDs, (b) CdSe/1CdS QDs, (c) CdSe/3CdS QDs and (d) CdSe/7CdS QDs measured by DLS.

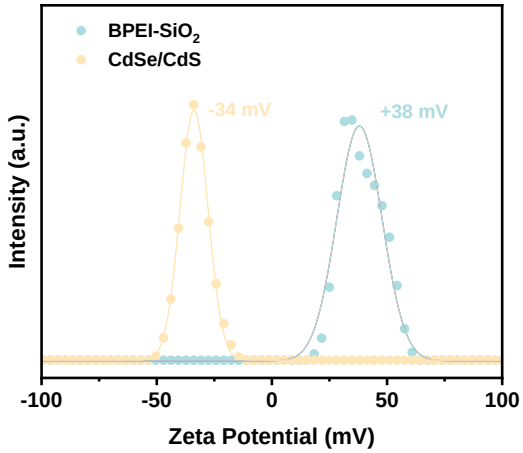

Fig. S3. Zeta potential (ξ) of BPEI-SiO_2 and CdSe/CdS QDs.

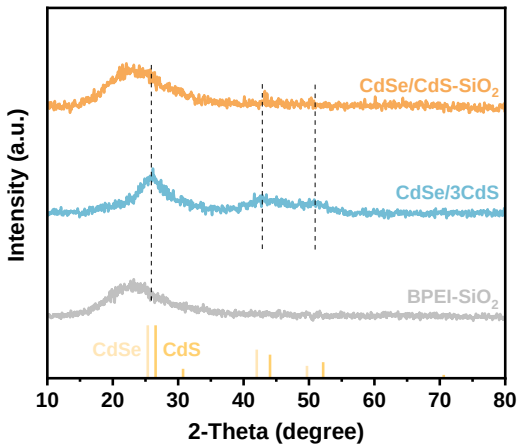

Fig. S4. XRD patterns of BPEI-SiO_2, CdS/3CdS QDs and CdSe/CdS-SiO_2 composite.

Note: In the XRD pattern of CdSe/CdS-SiO_2 composite, no discernible characteristic peaks associated with CdSe/3CdS QDs are observed, presumably due to their low content, nanoscale dimensions, and uniform dispersion throughout the composites.[2]

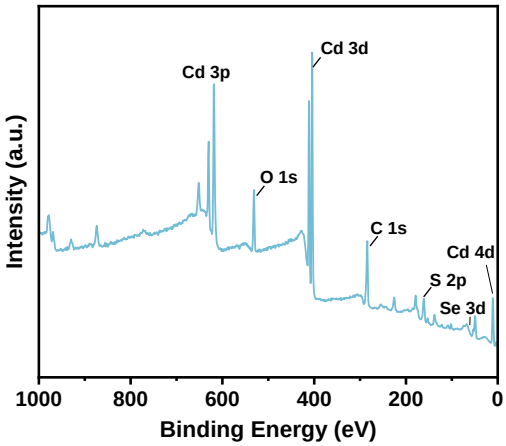

Fig. S5. XPS survey spectra of CdSe/CdS QDs.

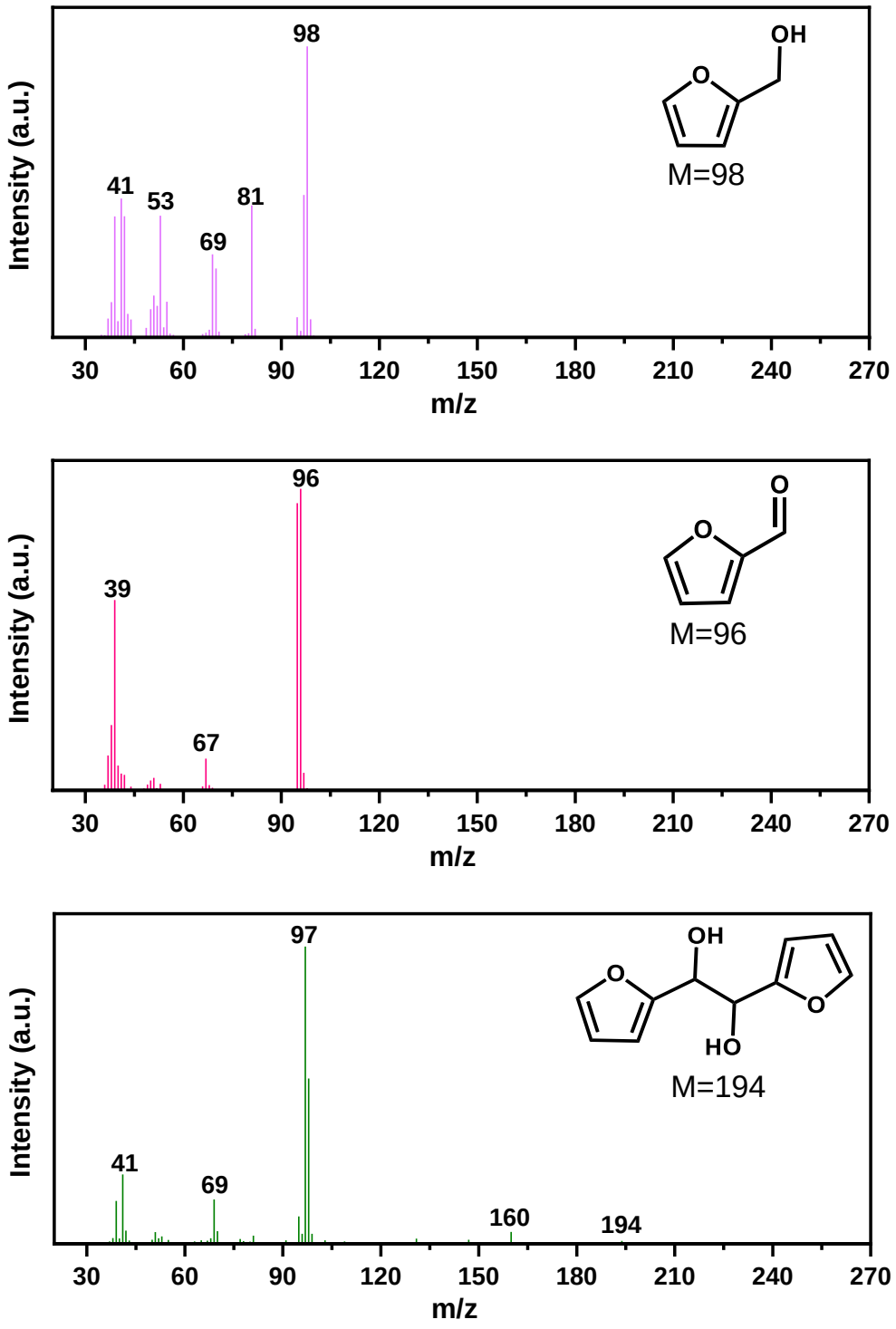

Fig. S6. Mass spectra of furfuryl alcohol (feedstock) and the obtained liquid products (furfural and hydrofurion).

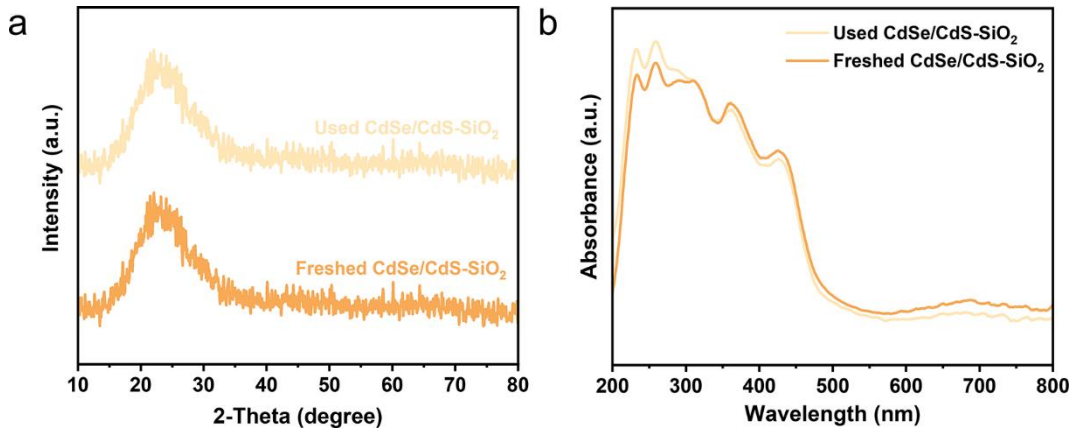

Fig. S7. (a) XRD patterns and (b) DRS spectra of fresh and used CdSe/CdS-SiO_2 composite.

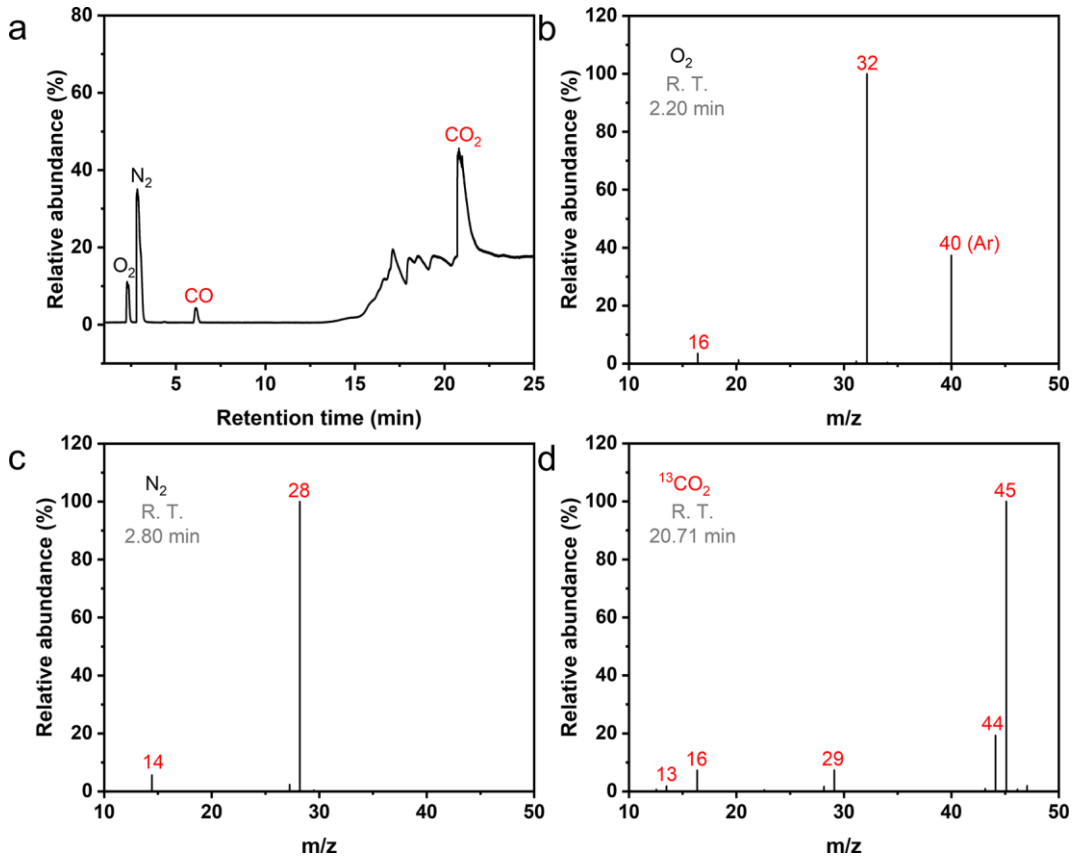

Fig. S8. (a) GC-MS analysis of CO_2 isotope tracing experiment using SH-Molecular Sieve 5A PLOT column and corresponding mass spectra of (b) O_2, (c) N_2 and (d) CO_2.

Note: As shown in **Fig. S8a**, O_2 (retention time (RT) at 2.20 min), N_2 (RT at 2.80 min), CO (RT at 5.99 min), and CO_2 (RT at 20.71 min) elute from SH-Molecular Sieve 5A PLOT one by one and generate the corresponding mass spectra (**Fig. S8b-d** and **Fig. 3g**), which match the standard mass spectra presented in the literature.[3] This demonstrates that the majority of CO originates from the photoreduction of labeled $^{13}CO_2$. Additionally, the peak with a low intensity and a m/z value of 44 ($^{12}CO_2$) in **Fig. S8d** derives from the decomposition of carbon residues on the catalyst surface.

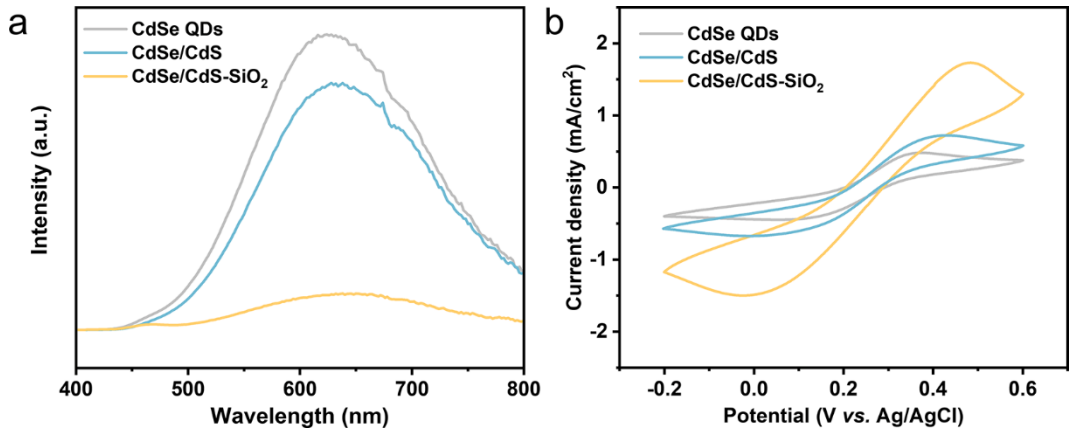

Fig. S9. (a) Steady-state PL emission spectra and (b) CV curves of CdSe QDs, CdSe/CdS QDs and CdSe/CdS-SiO_2 composite.

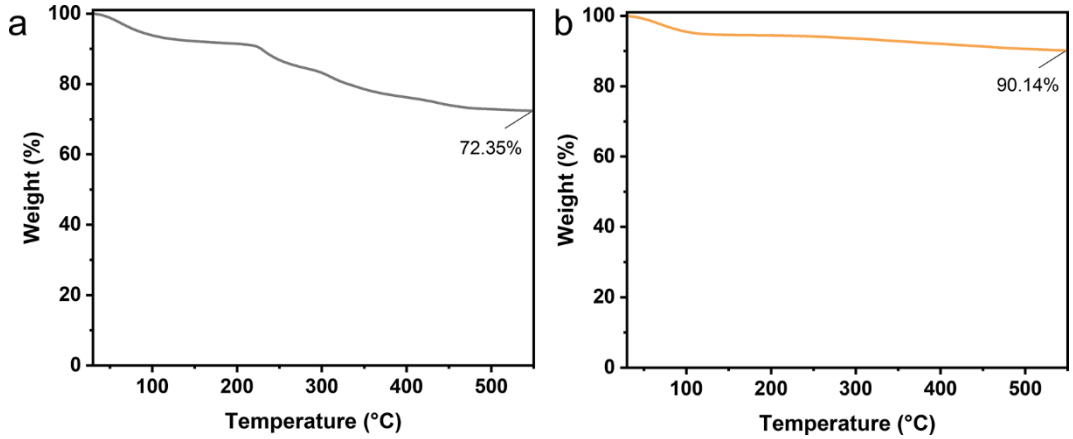

Fig. S10. TG curves of (a) CdSe/CdS QDs and (b) CdSe/CdS-SiO_2 composite.

Note: As displayed in **Fig. S10b**, the CdSe/CdS-SiO_2 sample exhibits a weight loss of only 9.86% when heated to 550 ℃, primarily due to the removal of adsorbed and coordinated water. This indicates that CdSe/CdS-SiO_2 composite possesses excellent thermal stability, making it suitable for TPD experiments without thermal decomposition.[4] In contrast, CdSe/CdS QDs experience a significant mass loss of 27.65% at 550 ℃, rendering them unsuitable for subsequent CO desorption experiments. Consequently, the CdSe-SiO_2 composite and CdSe/CdS-SiO_2 composite are chosen as the preferred samples in the CO_2 adsorption and CO desorption experiments.

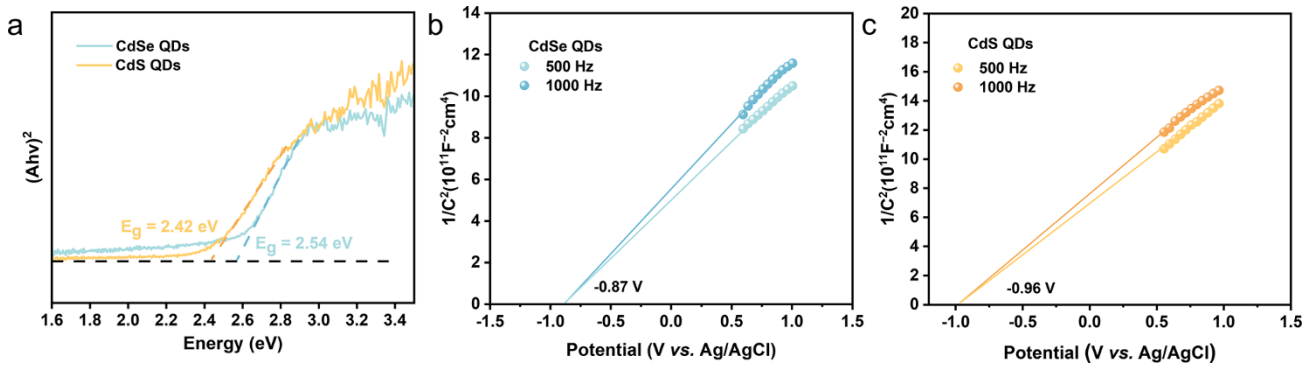

Fig. S11. (a) Tauc plots of CdSe and CdS QDs. Mott-Schottky plots of (b) CdSe QDs and (c) CdS QDs.

Note: The band gap energy of CdSe and CdS QDs was calculated based on the following formula:[5]

$$(Ahν)^n = K \cdot (hν - E_g)$$

In this equation, A represents the absorption coefficient, hν denotes the photon energy, K is a constant, E_g corresponds to the band gap energy, n is related to the type of semiconductor. Notably, CdSe and CdS are direct band gap semiconductors with n = 2. As shown in **Fig. S11a**, the E_g values evaluated for CdSe and CdS QDs are 2.54 and 2.42 eV, respectively (the E_g value of CdSe QDs increases due to their small particle size).[6] Morever, based on Mott-Schottky analysis, the conduction band (CB) potentials of CdSe and CdS are estimated to be −0.87 and −0.96 V (*vs.* $E_{Ag/AgCl}$), respectively. When converted to the normal hydrogen electrode (NHE), using the equation $E_{NHE} = E_{Ag/AgCl} + 0.197$ at pH = 7, the CB potentials of CdSe and CdS are −0.67 and −0.76 V, respectively.[7] Consequently, the valence band potentials (*vs.* E_{NHE}) are calculated to be +1.87 and +1.66 V for CdSe and CdS, respectively, indicating the type-II band structure in CdSe/CdS core-shell QDs (**Fig. 5e**).[8, 9]

Table S1. The kinetic analysis of emission decay for CdSe QDs, CdSe/CdS QDs and CdSe/CdS-SiO_2 composite.

Catalyst	A_1 (%)	τ_1 (ns)	A_2 (%)	τ_2 (ns)	τ_a (ns)
CdSe QDs	0.62	4.94	0.53	58.39	53.54
CdSe/CdS QDs	1.15	3.25	0.51	41.13	35.37
CdSe/CdS-SiO_2	2.23	2.14	0.41	39.48	30.99

Note: The decay curves of the TRPL spectra are fitted with biexponential equation. The average emission lifetime (τ_a) reflecting the overall emission decay behavior of the sample, which is calculated based on the following equation:[10]

$$I(t) = A_1 \exp(-t/\tau_1) + A_2 \exp(-t/\tau_2)$$

$$\tau_a = \frac{A_1\tau_1^2 + A_2\tau_2^2}{A_1\tau_1 + A_2\tau_2}$$

where τ_1 and τ_2 are the emission lifetimes, and A_1 and A_2 are the corresponding amplitudes.

References

1 G. Liu, W. Liang, X. Xue, F. Rosei and Y. Wang, *Adv. Sci.*, 2021, **8**, 2102784.
2 M.-Y. Qi, Y.-H. Li, M. Anpo, Z.-R. Tang and Y.-J. Xu, *ACS Catal.*, 2020, **10**, 14327–14335.
3 S. Wang, B. Jiang, J. Henzie, F. Xu, C. Liu, X. Meng, S. Zou, H. Song, Y. Pan, H. Li, J. Yu, H. Chen and J. Ye, *Nat. Commun.*, 2023, **14**, 2534.
4 M.-Y. Qi and Y.-J. Xu, *Angew. Chem., Int. Ed.*, 2023, **62**, e202311731.
5 S. Qi, Y. Miao, J. Chen, H. Chu, B. Tian, B. Wu, Y. Li and B. Xin, *Nanomater.*, 2021, **11**, 1357.
6 Q. Guo, F. Liang, X.-B. Li, Y.-J. Gao, M.-Y. Huang, Y. Wang, S.-G. Xia, X.-Y. Gao, Q.-C. Gan, Z.-S. Lin, C.-H. Tung and L.-Z. Wu, *Chem*, 2019, **5**, 2605–2616.
7 A. P. Rangappa, D. Praveen Kumar, Y. Hong, S. Jeong, D. A. Reddy, J. K. Song and T. K. Kim, *ACS Appl. Energy Mater.*, 2020, **3**, 10533–10540.
8 Y. Nandan and M. S. Mehata, *Sci. Rep.*, 2019, **9**, 2.
9 S. Shenoy and K. Tarafder, *J. Phys.: Condens.Matter*, 2020, **32**, 275501.
10 C.-L. Tan, M.-Y. Qi, Z.-R. Tang and Y.-J. Xu, *ACS Catal.*, 2023, **13**, 8317–8329.